Non-centrosymmetric $Ce_3OCl[AsO_3]_2$

Hamdi Ben Yahia, Ute Ch. Rodewald, and Rainer Pöttgen

Institut für Anorganische und Analytische Chemie, Universität Münster, Corrensstraße 30,
48149 Münster, Germany

Reprint requests to R. Pöttgen. E-mail: pottgen@uni-muenster.de

Z. Naturforsch. **2009**, *64b,* 896 – 900; received May 6, 2009

The arsenite chloride $Ce_3OCl[AsO_3]_2$ was synthesized in the form of colorless crystals from arsenic and cerium dioxide in a NaCl / KCl flux at 850 °C. $Ce_3OCl[AsO_3]_2$ crystallizes with the non-centrosymmetric tetragonal $Gd_3OCl[AsO_3]_2$ type, space group $P4_2nm$. The structure was refined from single crystal diffractometer data: $a = 12.8590(6)$, $c = 5.5627(3)$ Å, $wR2 = 0.0429$, 1463 F^2 values, and 65 variables. The structure is built up from chains of *trans* edge-sharing $OCe_{4/2}$ tetrahedra. The $[AsO_3]^{3-}$ units coordinate to these chains *via* the oxygen atoms. Their lone-pairs point all to a common channel. Formation of the non-centrosymmetric superstructure is most likely driven by geometrical constraints and is discussed on the basis of a group-subgroup scheme.

Key words: Oxoarsenite, Rare Earth Compound, Crystal Structure

Introduction

Eutectic salt flux systems [1, 2] are a useful preparative tool in solid-state chemistry to (i) offer mild synthesis conditions at comparatively low reaction temperatures, and to (ii) provide a solvent which favors the growth of single crystals for structure determination and property investigations. We have repeatedly used these fluxes for the growth of *RETPn*O (*RE* = rare earth element; *T* = late transition metal; *Pn* = P, As, Sb) pnictide oxide crystals with the tetragonal ZrCuSiAs- or rhombohedral NdZnPO-type structures [3 – 9], in order to investigate the optical and magnetic properties of these fascinating materials.

Compared to tin flux syntheses, as realized for the phosphide oxides Ce*T*PO (*T* = Fe, Ru, Os) [10, 11], the halide fluxes often lead to side reactions, incorporating the halide from the flux. While large single crystals have been obtained for the series of phosphide oxides *RE*ZnPO [5, 6] and arsenide oxides *RE*ZnAsO [9], the salt flux synthesis of PrRuAsO in alumina crucibles revealed the side product $Pr_5O_4Cl[AsO_3]_2$ [12]. Recent attempts to obtain ZrCuSiAs-type materials with trivalent europium *via* NaCl / KCl fluxes gave well shaped crystals of the apatite $Eu_5[PO_4]_3Cl$ [13]. Herein we report on another side product, $Ce_3OCl[AsO_3]_2$, which is isotypic with $Gd_3OCl[AsO_3]_2$ [14], and structurally closely related to $La_3OCl[AsO_3]_2$ [15], and on an alternative synthesis strategy and the group-subgroup relations between the structures of $La_3OCl[AsO_3]_2$ and $Ce_3OCl[AsO_3]_2$.

Table 1. Crystal data and structure refinement for $Ce_3OCl[AsO_3]_2$.

Composition		$Ce_3OCl[AsO_3]_2$
Molar mass, g mol^{-1}		717.65
Crystal size, μm^3		20 × 50 × 140
Formula units / cell Z		4
Unit cell dimensions		
a, pm		1285.90(6)
c, pm		556.27(3)
V, nm^3		0.9198
Calculated density, g/cm^3		5.18
Absorption coefficient, mm^{-1}		22.0
F(000), e		1252
θ range, deg		2 – 32
Detector distance, mm		90
Exposure time, min		5
ω range; increment, deg		0 – 180; 1.0
Integr. param. A, B, EMS		12.0; 2.0; 0.012
Range in *hkl*		±18, ±18, ±7
Total no. of reflections		19256
Transm. ratio (max / min)		0.624 / 0.206
	subcell	superstructure
Space group	$P4_2/mnm$	$P4_2nm$
Independent reflections / R_{int}	805 / 0.0389	1463 / 0.0380
Refl. with $I \geq 2\sigma(I)$ / R_{sigma}	766 / 0.0147	1382 / 0.0191
Data / parameters	805 / 38	1463 / 65
$R1/wR2$ for $I \geq 2\sigma(I)$	0.0668 / 0.1815	0.0181 / 0.0424
$R1/wR2$ for all data	0.0690 / 0.1822	0.0204 / 0.0429
BASF	–	0.55(3)
Goodness-of-fit on F^2	1.442	0.981
Extinction coefficient	0.0079(8)	0.0062(2)
Largest diff. peak / hole, e Å^{-3}	5.19 / −5.06	0.96 / −1.08

Atom	Site	x	y	z	U_{eq}/U_{iso}
subcell, space group $P4_2/mnm$					
Ce1	$4f$	0.27160(11)	x	0	63(5)
Ce2	$8i$	0.13659(11)	0.55325(11)	0	83(5)
As	$8i$	0.9824(2)	0.2079(2)	0	86(6)
Cl	$8j$	0.1663(7)	x	0.456(2)	183(28)
O1	$4d$	0	1/2	1/4	52(43)
O2	$8i$	0.0906(17)	0.2902(19)	0	290(64)
O3	$16k$	0.9166(11)	0.2752(11)	0.235(3)	119(26)
superstructure, space group $P4_2nm$					
Ce1	$4c$	0.27173(2)	x	0.00001(9)	58(1)
Ce2	$8d$	0.13659(2)	0.55335(2)	0.02094(4)	71(1)
As	$8d$	0.98258(3)	0.20786(3)	0.99721(14)	71(1)
Cl	$4c$	0.16624(11)	x	0.4702(4)	211(4)
O1	$4b$	0	1/2	0.2665(14)	91(8)
O2	$8d$	0.0905(3)	0.2908(3)	0.9685(8)	155(9)
O3	$8d$	0.9225(5)	0.2742(5)	0.2425(8)	112(10)
O4	$8d$	−0.9104(5)	−0.2759(5)	−0.2298(9)	89(9)

Table 2. Atom positions and equivalent isotropic displacement parameters (pm^2) for the subcell and the superstructure of $Ce_3OCl[AsO_3]_2$. U_{eq} is defined as one third of the trace of the orthogonalized U_{ij} tensor. In the subcell refinement the chlorine site was refined with a split position and half occupancy on the $8j$ site.

Experimental Section

Synthesis

The title compound was prepared by solid state reaction from a mixture of arsenic (Sigma-Aldrich, 99.999 %), cerium dioxide (Chempur, $>$ 99.99 %) and a NaCl (Merck, $>$ 99.5 %) / KCl (Chempur, 99.9 %) salt flux (1 : 1 molar ratio) with a 4 : 1 : 34 molar ratio, respectively. The arsenic was purified by fractional sublimation [9] under vacuum prior to use. The mixture was put in a silica tube which was sealed under vacuum. The tube was heated at 500 °C for 6 h and at 850 °C for 72 h. By decreasing the temperature at a rate of 10 °C/h to r. t. we obtained colorless crystals of $Ce_3O[AsO_3]_2Cl$ besides unreacted CeO_2.

EDX data

Semiquantitative EDX analyses of different single crystals including the one investigated on the diffractometer (Fig. 1) were carried out with a Leica 420i scanning electron microscope using CeO_2, InAs and KCl as standards. The experimentally observed compositions were close to the ideal one. No impurity elements heavier than sodium (detection limit of the instrument) were observed.

X-Ray diffraction

The polycrystalline sample was characterized by a Guinier pattern (imaging plate detector, Fujifilm BAS-1800) with $CuK_{\alpha1}$ radiation and α-quartz (a = 4.9130, c = 5.4046 Å) as an internal standard. The diffractogram showed mainly reflections of still unreacted fluorite-type cerium dioxide CeO_2 ($Fm\bar{3}m$, a = 5.41 Å) besides weak reflections of the title compound.

The CeO_2 and the crystals of $Ce_3O[AsO_3]_2Cl$ could easily be distinguished by their shape. A crystal suitable for single-crystal X-ray diffraction was selected on the basis of the size and the sharpness of the diffraction spots by Laue photographs on a Buerger camera (using white Mo radiation). The data collection was carried out on a Stoe IPDS II diffractometer using MoK_α radiation. Data processing and first refinements were performed with the JANA2006 program package [16]. A Gaussian-type absorption correction was applied, and the shape of the crystal was determined with the video microscope of the Stoe CCD. Details about data collection and refinement are summarized in Table 1.

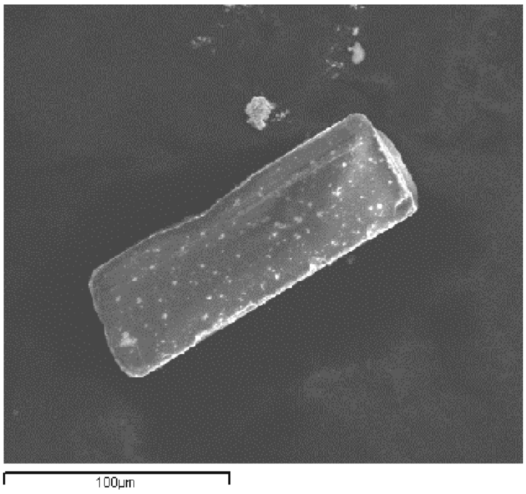

Fig. 1. SEM image of the $Ce_3OCl(AsO_3)_2$ single crystal used for the XR data collection.

Structure refinement

Careful examination of the $Ce_3O[AsO_3]_2Cl$ data set revealed a primitive tetragonal unit cell with high Laue symmetry and extinction conditions ($00l$ only observed for $l = 2n$, $h00$ only for $h = 2n$) leading to the space groups $P4_2/mnm$ and $P4_2nm$, of which the non-centrosymmetric group was

Table 3. Anisotropic displacement parameters (pm^2) for the superstructure of $Ce_3OCl[AsO_3]_2$. The anisotropic displacement factor exponent takes the form: $-2\pi^2[(ha^*)^2U_{11} + \ldots + 2hka^*b^*U_{12}]$.

Atom	U_{11}	U_{22}	U_{33}	U_{12}	U_{13}	U_{23}
Ce1	57(1)	U_{11}	60(2)	18(1)	−1(1)	U_{13}
Ce2	66(1)	72(1)	73(1)	−4(1)	1(1)	1(1)
As	81(2)	62(2)	69(2)	−1(1)	3(3)	7(2)
Cl	185(5)	U_{11}	263(12)	90(6)	30(6)	U_{13}
O1	129(41)	29(36)	113(22)	−22(41)	0	0
O2	71(14)	203(17)	190(24)	−50(12)	−29(15)	74(16)
O3	119(24)	147(26)	70(18)	22(18)	24(14)	−27(15)
O4	82(21)	108(23)	79(16)	−18(17)	21(13)	−10(15)

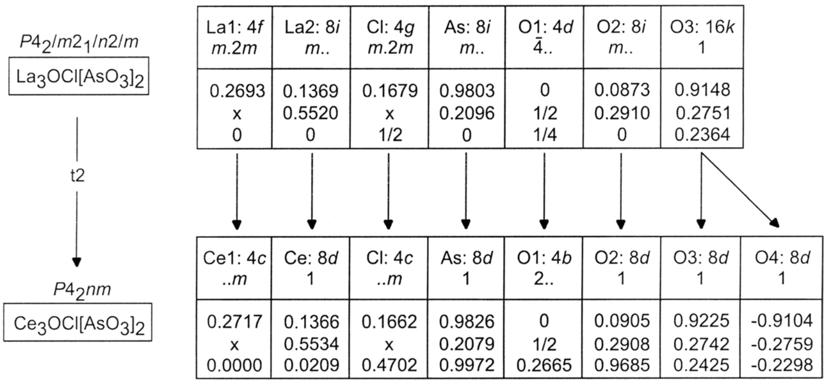

La1: 4*f* *m.2m*	La2: 8*i* *m..*	Cl: 4*g* *m.2m*	As: 8*i* *m..*	O1: 4*d* $\bar{4}$..	O2: 8*i* *m..*	O3: 16*k* 1
0.2693 x 0	0.1369 0.5520 0	0.1679 x 1/2	0.9803 0.2096 0	0 1/2 1/4	0.0873 0.2910 0	0.9148 0.2751 0.2364

Ce1: 4*c* *..m*	Ce: 8*d* 1	Cl: 4*c* *..m*	As: 8*d* 1	O1: 4*b* 2..	O2: 8*d* 1	O3: 8*d* 1	O4: 8*d* 1
0.2717 x 0.0000	0.1366 0.5534 0.0209	0.1662 x 0.4702	0.9826 0.2079 0.9972	0 1/2 0.2665	0.0905 0.2908 0.9685	0.9225 0.2742 0.2425	-0.9104 -0.2759 -0.2298

Fig. 2. Group-subgroup scheme in the Bärnighausen formalism [20–22] for the structures of $La_3OCl[AsO_3]_2$ [15] and $Ce_3OCl[AsO_3]_2$. The index for the *translationengleiche* symmetry reduction (t) and the evolution of the atomic parameters is given.

found to be correct during structure refinement. Nevertheless, the structure was first solved in the centro-symmetric group $P4_2/mnm$. Most of the atomic positions were located using the superflip program implemented in the JANA2006 package [16]. The use of difference Fourier syntheses allowed us to localize the remaining oxygen atom positions. Inspection of the data bases then readily revealed the structural relationship with $La_3OCl[AsO_3]_2$ [15] and $Gd_3OCl[AsO_3]_2$ [14]. The structure was then refined with SHELXL-97 [17] (full-matrix least-squares on F^2) with anisotropic atomic displacement parameters (APDs) for all atoms. The 4*g* chlorine site showed a very large U_{33} parameter, and subsequently this site was refined with a split position *x x z* instead of *x x* 1/2, and with an isotropic displacement parameter, leading to the parameters listed in Table 1. The residuals of this centrosymmetric refinement were enhanced and also the residual electron densities were not satisfactory. These parameters and the split position for the chlorine site were a strong hint for superstructure formation upon loss of inversion symmetry, similar to $Gd_3OCl[AsO_3]_2$ [14].

Subsequently we precalculated the sites for the non-centrosymmetric space group $P4_2nm$ and refined the structure again. Now we gained free *z* parameters and an additional oxygen site through splitting of the 16*k* site in the superstructure (Fig. 2). The refinement then smoothly converged to the residuals listed in Table 1 with well-behaved displacements for all sites. Calculation of the Flack parameter [18, 19] indicated twinning by inversion (caused by the *translationengleiche* transition from $P4_2/mnm$ to $P4_2nm$). Finally the structure was refined as an inversion twin. The refined atomic positions for the subcell and the superstructure and the ADPs for the superstructure are given in Tables 2 and 3, respectively.

Further details of the crystal structure investigation may be obtained from Fachinformationszentrum Karlsruhe, 76344 Eggenstein-Leopoldshafen, Germany (fax: +49-7247-808-666; e-mail: crysdata@fiz-karlsruhe.de, http://www.fiz-informationsdienste.de/en/DB/icsd/depot_anforderung.html) on quoting the deposition number CSD-420652.

Discussion

The arsenite chloride $Ce_3OCl[AsO_3]_2$ is isotypic with the recently reported gadolinium compound [14]. These two structures crystallize with the non-centrosymmetric space group $P4_2nm$, while $La_3OCl[AsO_3]_2$ [15] adopts the centrosymmetric space group $P4_2/mnm$. Due to the lanthanide contraction, the cell parameters decrease from the lanthanum to the gadolinium compound.

The transition from a centrosymmetric to a non-centrosymmetric structure for such an ionic compound is most likely driven by geometrical effects. The cerium atoms are already slightly too small to enable the centrosymmetric variant. As emphasized in the Bärnighausen tree [20–22] in Fig. 2, we gain free *z* parameters, and the 16*k* O3 position splits into two eightfold sites 8*d*. The slight puckering then enables a

Table 4. Interatomic distances (in Å), angles (in deg) and bond valence sums (BVSs with coordination numbers in brackets) for $Ce_3O(AsO_3)_2Cl$.

	Distance	BV[a]		Distance	BV
Ce1–O2(×2)	2.351(3)	0.582	As–O2	1.757(3)	1.090
Ce1–O4(×2)	2.411(6)	0.495	As–O3	1.784(5)	1.014
Ce1–O3(×2)	2.482(5)	0.409	As–O4	1.795(6)	0.984
	⟨2.415⟩	BVS [6] = 2.972		⟨1.779⟩	BVS [3] = 3.088
Ce1–Cl	3.244(2)	0.141			
Ce1–Cl	3.517(2)	0.068		angle	
		BVS [8] = 3.181	O2–As–O3	97.0(2)	
Ce2–O1	2.329(5)	0.618	O2–As–O4	92.8(2)	
Ce2–O1	2.358(5)	0.572	O3–As–O4	94.6(3)	
Ce2–O3	2.559(5)	0.332		⟨94.8⟩	
Ce2–O4	2.563(6)	0.328			
Ce2–O3	2.648(6)	0.261			
Ce2–O4	2.670(6)	0.246			
Ce2–O2	2.702(4)	0.226			
		BVS [7] = 2.583			
Ce2–Cl	2.935(1)	0.326			
		BVS [8] = 2.909			

[a] BV = $e^{(r0-r)/b}$ with the following parameters: $b = 0.37$, r_0 (Ce–O) = 2.151, r_0 (As^{III}–O) = 1.789, r_0 (As^{III}–Cl) = 2.16, and r_0 (Ce–Cl) = 2.52 Å [23, 24].

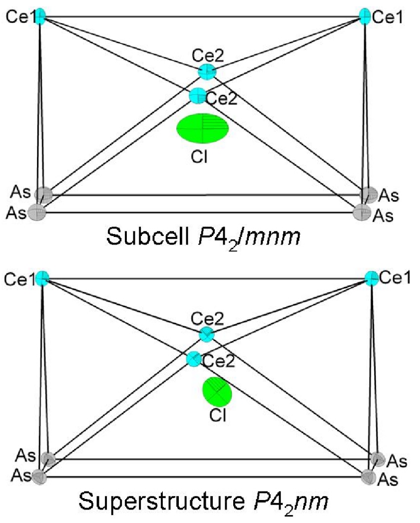

Fig. 3. Coordination of the chlorine atoms in the centrosymmetric (top) and non-centrosymmetric (bottom) models of the $Ce_3OCl(AsO_3)_2$ structure. For details see text.

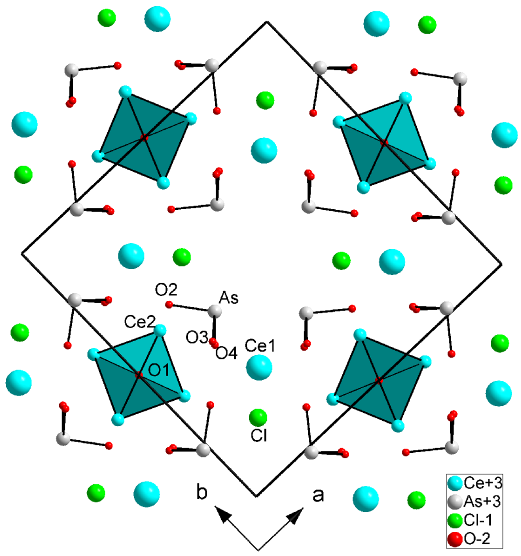

Fig. 4. Projection of the $Ce_3OCl(AsO_3)_2$ structure along the short unit cell axis. The chains of *trans*-edge-sharing $OCe_{4/2}$ tetrahedra and the $[AsO_3]^{3-}$ units are emphasized.

similar atomic arrangement, however, with lower symmetry. The largest shift occurs for the chlorine site. Upon superstructure formation, the chlorine atom is displaced off the center of a dicapped trigonal prism formed by the cerium and arsenic atoms (Fig. 3).

A projection of the $Ce_3OCl[AsO_3]_2$ structure along the short unit cell axis is presented in Fig. 4. The structure contains two striking structural motifs. The O1 atoms have tetrahedral cerium coordination, and these tetrahedra share adjacent edges, leading to infinite chains running along $1/2\ 0\ z$. The Ψ^1-tetrahedral $[AsO_3]^{3-}$ units coordinate to these strands *via* the oxygen atoms. The As–O distances range from 176 to 180 pm, similar to the data of $La_3OCl[AsO_3]_2$ [15] and $Gd_3OCl[AsO_3]_2$ [14]. The lone pairs of the arsenite units all point into a common channel.

Since the crystals are colorless, an ionic formula splitting $(3Ce^{3+})O^{2-}Cl^-(2AsO_3^{3-})$ is adequate. The interatomic distances and coordinations lead to the bond valence sums [23] listed in Table 4 which are in good agreement with the salt-like formulation. For further crystal chemical details we refer to the original work on $La_3OCl[AsO_3]_2$ [15].

Finally, one might think of a high-temperature ($Ce_3OCl[AsO_3]_2$) or high-pressure ($La_3OCl[AsO_3]_2$)

phase transition between the centrosymmetric and the non-centrosymmetric variants. Such investigations, however, can only be performed under *in situ* conditions, since the phase transition is of a displacive type.

Acknowledgements

This work was financially supported by the Deutsche Forschungsgemeinschaft. H. B. Y. is indebted to the Alexander von Humboldt Foundation for a research stipend.

---

[1] G. Brauer, *Handbuch der Präparativen Anorganischen Chemie*, 3. Band, 4. Abschnitt, 3. Aufl., Enke, Stuttgart, **1975**.

[2] W. Sundermeyer, *Angew. Chem.* **1964**, *77*, 241.

[3] D. Johrendt, R. Pöttgen, *Angew. Chem.* **2008**, *120*, 4860; *Angew. Chem. Int. Ed.* **2008**, *47*, 4782.

[4] R. Pöttgen, D. Johrendt, *Z. Naturforsch.* **2008**, *63b*, 1135.

[5] H. Lincke, T. Nilges, R. Pöttgen, *Z. Anorg. Allg. Chem.* **2006**, *632*, 1804.

[6] H. Lincke, R. Glaum, V. Dittrich, M. Tegel, D. Johrendt, W. Hermes, M. H. Möller, T. Nilges, R. Pöttgen, *Z. Anorg. Allg. Chem.* **2008**, *634*, 1339.

[7] I. Schellenberg, T. Nilges, R. Pöttgen, *Z. Naturforsch.* **2008**, *63b*, 834.

[8] M. Tegel, I. Schellenberg, R. Pöttgen, D. Johrendt, *Z. Naturforsch.* **2008**, *63b*, 1057.

[9] H. Lincke, R. Glaum, V. Dittrich, M.H. Möller, R. Pöttgen, *Z. Anorg. Allg. Chem.* **2009**, *635*, 936.

[10] E.M. Brüning, C. Krellner, M. Baenitz, A. Jesche, F. Steglich, C. Geibel, *Phys. Rev. Lett.* **2008**, *101*, 117206.

[11] C. Krellner, N. S. Kini, E. M. Brüning, K. Koch, H. Rosner, M. Nicklas, M. Baenitz, C. Geibel, *Phys. Rev. B* **2007**, *76*, 104418.

[12] H. Ben Yahia, U. Ch. Rodewald, T. Schleid, R. Pöttgen, unpublished results.

[13] H. Ben Yahia, U. Ch. Rodewald, R. Pöttgen, *Z. Naturforsch.* **2009**, *64b*, 577.

[14] D.-H. Kang, Th. Komm, T. Schleid, *Z. Kristallogr.* **2005**, *Suppl. 22*, 157.

[15] D.-H. Kang, T. Schleid, *Z. Anorg. Allg. Chem.* **2007**, *633*, 1205.

[16] V. Petříček, M. Dušek, L. Palatinus, JANA2006, The Crystallographic Computing System, Institute of Physics, University of Prague, Prague (Czech Republic) **2006**.

[17] G.M. Sheldrick, SHELXL-97, Program for Crystal Structure Refinement, University of Göttingen, Göttingen (Germany) **1997**.

[18] H.D. Flack, G. Bernadinelli, *Acta Crystallogr.* **1999**, *A55*, 908.

[19] H.D. Flack, G. Bernadinelli, *J. Appl. Crystallogr.* **2000**, *33*, 1143.

[20] H. Bärnighausen, *Commun. Math. Chem.* **1980**, *9*, 139.

[21] H. Bärnighausen, U. Müller, *Symmetriebeziehungen zwischen den Raumgruppen als Hilfsmittel zur straffen Darstellung von Strukturzusammenhängen in der Kristallchemie*, University of Karlsruhe and University/GH Kassel, **1996**.

[22] U. Müller, *Z. Anorg. Allg. Chem.* **2004**, *630*, 1519.

[23] I.D. Brown, D. Altermatt, *Acta Crystallogr. B* **1985**, *41*, 244.

[24] N.E. Brese, M. O'Keeffe, *Acta Crystallogr. B* **1991**, *47*, 192.